

# Advances in the simulation and automated measurement of well-sorted granular material:

## 1. Simulation

D. Buscombe<sup>1</sup> and D. M. Rubin<sup>2</sup>

Received 24 January 2011; revised 26 January 2012; accepted 30 January 2012; published 3 April 2012.

[1] In this, the first of a pair of papers which address the simulation and automated measurement of well-sorted natural granular material, a method is presented for simulation of two-phase (solid, void) assemblages of discrete non-cohesive particles. The purpose is to have a flexible, yet computationally and theoretically simple, suite of tools with well constrained and well known statistical properties, in order to simulate realistic granular material as a discrete element model with realistic size and shape distributions, for a variety of purposes. The stochastic modeling framework is based on three-dimensional tessellations with variable degrees of order in particle-packing arrangement. Examples of sediments with a variety of particle size distributions and spatial variability in grain size are presented. The relationship between particle shape and porosity conforms to published data. The immediate application is testing new algorithms for automated measurements of particle properties (mean and standard deviation of particle sizes, and apparent porosity) from images of natural sediment, as detailed in the second of this pair of papers. The model could also prove useful for simulating specific depositional structures found in natural sediments, the result of physical alterations to packing and grain fabric, using discrete particle flow models. While the principal focus here is on naturally occurring sediment and sedimentary rock, the methods presented might also be useful for simulations of similar granular or cellular material encountered in engineering, industrial and life sciences.

**Citation:** Buscombe, D., and D. M. Rubin (2012), Advances in the simulation and automated measurement of well-sorted granular material: 1. Simulation, *J. Geophys. Res.*, 117, F02001, doi:10.1029/2011JF001974.

## 1. Introduction

### 1.1. Motivation

[2] This is the first of a pair of papers (the second being *Buscombe and Rubin* [2012, hereinafter, part 2]) on the particle-scale structure of natural granular material (sediment), in which a new approach to the three-dimensional simulation of such materials has been developed principally in order to meet the needs of two expanding research areas, namely: 1) automated methods for in situ sampling of granular properties from images of sediment; and 2) the development of discrete particle models for investigating the physics of granular and fluid-granular flows.

[3] Measurements of granular properties from images of planar sections through volumes of intact consolidated granular material [e.g., *Fara and Scheidegger*, 1961; *Preston and Davis*, 1976; *Lin*, 1982; *Tovey and Hounslow*, 1995; *Prince et al.*, 1995; *Van den Berg et al.*, 2002; *Neupauer and Powell*, 2005; *Torabi et al.*, 2008] and unconsolidated

granular surfaces and vertical sections [e.g., *Rubin*, 2004; *Carbonneau et al.*, 2004; *Graham et al.*, 2005; *Buscombe*, 2008; *Buscombe and Masselink*, 2009; *Warrick et al.*, 2009; *Buscombe et al.*, 2010] are designed to give rapid yet highly accurate estimates of sediment structure (for example, packing, porosity, and dominant orientation) and particle properties (principally, particle size, shape, concentration, packing) in the field and laboratory. The goal is to estimate particle size statistics in situ using images of the surface of sediment which is interacting with fluid flows at a given instant in time. In particular, these techniques have the potential to allow much more dense sampling and analysis of sediment in the field. Such information aids the remote characterization of the sea or river bed in between stages of motion [*Barnard et al.*, 2007; *Rubin et al.*, 2010]. These advances may also allow imaging to replace or to be used in conjunction with more traditional surface-sampling procedures for sands such as epoxy peels for vertical sections [e.g., *Gretzen and Levey*, 1982] and petroleum jelly cards [e.g., *Ingle*, 1966].

[4] The lack of a robust particle-size standard for validating measurements from such imagery arises due to the fact that, in a plan view image of a granular material, as the geometric projection of a 3D surface onto a 2D plane (such as those in Figure 1), particles overlap (parts of particles are sitting on top of others, wholly or partially obscuring those underneath). There are no visible voids, only visible

<sup>1</sup>School of Marine Science and Engineering, University of Plymouth, Plymouth, UK.

<sup>2</sup>United States Geological Survey, Santa Cruz, California, USA.

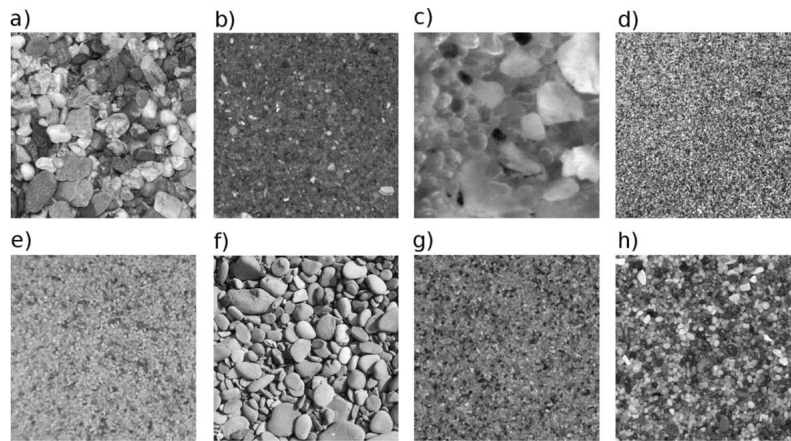


**Figure 1.** Example images of the surfaces of well-sorted natural sediment from 8 distinct populations from fluvial, coastal and shelf environments, with particle sizes ranging from silt to cobble.

surface and parts of subsurface particles. Therefore, neither measurements of the diameters of completely visible particles nor bulk measurements of the surface layers such as sieving are appropriate metrics against which to evaluate the performance of direct statistical estimates of particle properties which use information from the entire image [Rubin, 2004; Buscombe *et al.*, 2010; Carbonneau *et al.*, 2004, 2005]. For a comprehensive review of the development of these statistical methods, as well as alternative methodologies which use thresholding techniques to isolate individual particles, the reader is referred to Buscombe *et al.* [2010].

[5] Motivated by this problem of evaluating statistical image processing methods for particle sizing, the solution of Barnard *et al.* [2007] and Buscombe *et al.* [2010] was to validate their respective measurement techniques by carrying out manual point counts of particle diameters on the screen. A regular grid was overlain on each image, and the intermediate diameters of every particle or partial particle lying at each grid intersection was measured. This method is satisfactory but laborious and therefore prohibitive of evaluating measurements from a very large set of images. In addition, in order to characterize the true population mean about 100 point count measurements are required for well sorted sands. This increases to an unknown number—possibly every particle in the image—if the entire distribution of sizes is to be characterized properly [Church *et al.*, 1987]. A final disadvantage of such an approach is that it inevitably introduces a fine bias in estimates of the population particle size statistics, by counting the partial axes of some particles. Therefore, some (as yet unknown) stereology is required which relates the size distribution of the axes of apparent particles comprising the surface to the actual distribution of diameters of those particles (this problem is considered further in part 2).

[6] Appropriate simulations of granular materials can readily overcome these disadvantages and therefore allow further progress in these measurement techniques. First and foremost, only simulated material can produce large sets of populations of particles quickly, with a range of specified particle size, particle shape, packing, porosity and other properties. Moreover, these properties can be known precisely, essential for the purposes of testing automated measurement approaches. In addition, such simulations can

provide a means by which to quantify the discrepancy between bulk particle size statistics and those derived from just the visible particles at the surface. Finally, the use of sediment models allow the total errors of measurement methods to be understood, for example by controlling optical aspects such as poor or uneven lighting, blur, distortion and poor resolution.

[7] Granular material is commonly modeled as discrete elements (grains), the interactions between which are exerted through contacts depending on boundary conditions and external forces applied, but also crucially on the way the grains are packaged (herein referred to by the common sedimentological term ‘packing’), and on the distribution of the sizes and shapes of the grains [Mehta, 2007]. Due to the structural complexities of many natural granular materials, it is useful to have algorithms capable of simulating particle assemblages which are idealized and have known or well constrained statistical properties, but which are also as realistic as possible. Such simulations are an essential component of many theoretical studies of granular physics [Mehta, 2007], forming the basis of studies into the static and kinematic properties of sediments. For example, simulating the micro-geometry of granular material aids the study of the flow of acoustic or electromagnetic energy (primarily optical and electrical), or water, through the material [e.g., Graton and Fraser, 1935; Bear, 1972; Tovey and Hounslow, 1995]. Such static simulations are therefore useful in many areas of sedimentary geology, especially the study of aquifers, and geophysical surveying. In addition, the simulation of realistic granular material made up of discrete particles is itself potentially useful in areas such as the direct numerical simulation of fluid-granular flows [e.g., Drake and Calantoni, 2001; Schmeeckle and Nelson, 2003], and a multitude of theoretical studies of granular properties for medical and chemical/industrial applications as well as geology and geophysics.

[8] Most numerical simulations of granular beds to date have invoked the use of spheres [e.g., Bernal and Mason, 1960; Jodrey and Tory, 1979; Moscinski and Bargiel, 1991] or ellipsoids [e.g., Potapov and Campbell, 1998; Favier *et al.*, 1999] of uniform or symmetrical size-distributions. However, natural particles such as sand can be modeled as convex polyhedra. That is to say, all interior angles are less than 180 degrees. Models which simulate particles as polyhedra

(in three dimensions) tend to generate a distribution of shapes [e.g., *Ghaboussi and Barbosa, 1990; Latham and Munjiza, 2004*]. However, they also tend to be computationally expensive and time-consuming due to the necessity for contact-detection algorithms [e.g., *Jensen et al., 1999*]. Moreover, little attention is generally paid to the realism of the size- and shape-distributions of the simulated material, and whether the quasi-crystalline structure of many natural particles, and the spectrum of interlocking arrangements (packing) are adequately simulated.

## 1.2. Objectives

[9] The principal objective of this paper is to develop methods to simulate sediments such as those in Figure 1, motivated by an observation that further development of techniques for automated measurement of such granular material is hampered by a lack of a true standard against which methods can be validated, as well as the laborious nature of these validation procedures. In doing so, a stochastic modeling framework has been developed which generates populations of particles which are qualitatively and quantitatively realistic, with a formalized yet simple mathematical framework, and with modest computing power. As such, this technique might find more general applicability in studies of granular packing and flows.

[10] In this contribution we develop a new approach to the simulation of three-dimensional populations of particles, packed into sediment beds. Both the individual particles and the bulk properties of the simulated granular material are realistic enough for application in the further development of automated estimation of particle properties, which is the subject of part 2. Therein, images of the planform of volumes of simulated particles aid the testing of new measurement techniques for the direct and completely automated estimate of the standard deviation of the distribution of particle sizes within an image of sediment. It is a direct estimate, with an analytical derivation, using only the information contained within the image in the frequency domain. As such the method closely follows *Buscombe et al. [2010]* who developed a similar method for mean particle size.

[11] *Buscombe et al. [2010]* developed a simple set of simulations of two-dimensional particle assemblages which allowed them to ascribe individual contributions to total error of an automated statistical algorithm for estimation of mean particle size caused by inter- and intraparticle shading. Significant advances have been made to that prototype model in the current contribution. These include an extension to three dimensions and a mathematical formalism of the modeling framework which allows the sediment to be simulated as a random field with known mathematical properties rather than vector drawings. This has allowed greater flexibility in simulating different particle packing, and a greater spectrum of possible size and shape distributions. The collective result is that the simulations, and therefore the images of their surfaces, are much more akin to natural granular material than those of *Buscombe et al. [2010]*.

## 2. Simulation of Granular Material

[12] The approach taken in this contribution is to simulate assemblages of individual discrete solid particles (granular material) which arise from a statistical continuum, namely

the Voronoi tessellation (defined below) of a point distribution. Each point in this distribution is therefore a particle center, and each vertex of the surrounding Voronoi cell is a closed particle boundary. Structural features of the resulting assemblage of particles (granular material), such as packing and distributions of size, are thus emergent properties of the relative location of the particle centers.

[13] The basic method is to generate a spatial distribution of points in 3D whose Voronoi tessellation produces cells which have the essential intrinsic properties of realistic particles. After formally introducing the suitability of the Voronoi tessellation as an analog for a collection of granular particles (section 2.1), given the innumerable means by which the distribution of particle centers might be realized, we necessarily consider only a few examples of point-generating processes and their resulting granular materials (section 2.2). Two basic classifications as considered, namely 1) conforming to an algorithm (a spatial point process; section 2.2.1) or 2) based on a discrete random field (section 2.2.2).

### 2.1. The Modified Voronoi Tessellation as a Model for Natural Particles

[14] Consider a non-cohesive granular material represented as a composite body composed of two phases: particles (solids) and voids (pores), occupying differing spatial positions ( $x$ , i.e., no particle overlap). The characteristic function of a two-phase (particle  $p$ , pore or void  $v$ ) body of bulk volume  $\forall$  with sub-volumes  $\forall_p$  and  $\forall_v$  is defined as [e.g., *Sen, 1984*]:

$$I(x) = \begin{cases} 1 & x \in \forall_p \\ 0 & x \in \forall_v \end{cases} \quad (1)$$

where  $x$  might be a pixel (for a granular material simulated in 2D) or a voxel (for a 3D material, the default used in this study unless otherwise stated). Only the solid phase is simulated. Void fraction is therefore  $\phi = \forall_v/\forall$ . Therefore the spatial distribution of the void phase—the pore space network—is an emergent property of the simulation of the solid phase.

[15] In a three-dimensional region  $\Omega$  consisting of points (particle centers)  $\{z_m\}_{m=1}^M$ ,  $\mathbb{R}_m$  is defined as the set in  $\Omega$  consisting of those points which are closer to  $z_m$  than any other  $z_n$ :

$$\mathbb{R}_m = x \in \Omega, |x - z_m| < |x - z_n|, \quad (2)$$

where  $n = 1, \dots, N(n \neq m)$  and  $m = 1, \dots, M$ . Given a point density  $\nu$ , the centroids (or ‘centers of mass’) of  $\mathbb{R}_m$  are defined by:

$$z_m^* = \frac{1}{|\mathbb{R}_m|} \int_{\mathbb{R}_m} x \nu(x) dx. \quad (3)$$

[16] The set of regions  $\{\mathbb{R}_m\}_{m=1}^M$  are called Voronoi cells. In this study  $\Omega$  is always the unit cube (or unit square for 2D simulations), therefore  $\nu$  is defined by the number of particles required,  $M$ . The Voronoi tessellation is analogous to the simultaneous ‘growth’ of particles in 3 dimensions, each from a point outwards in all directions at an identical rate. Particles which intersect with the boundary of  $\Omega$  are removed.

[17] The Voronoi tessellation creates only the solid phase  $\forall_p$ . Pore space  $\forall_v$ , is created by stopping particle ‘growth’ at a user-defined  $\phi$ . A porosity of  $\phi = 0$  would therefore allow

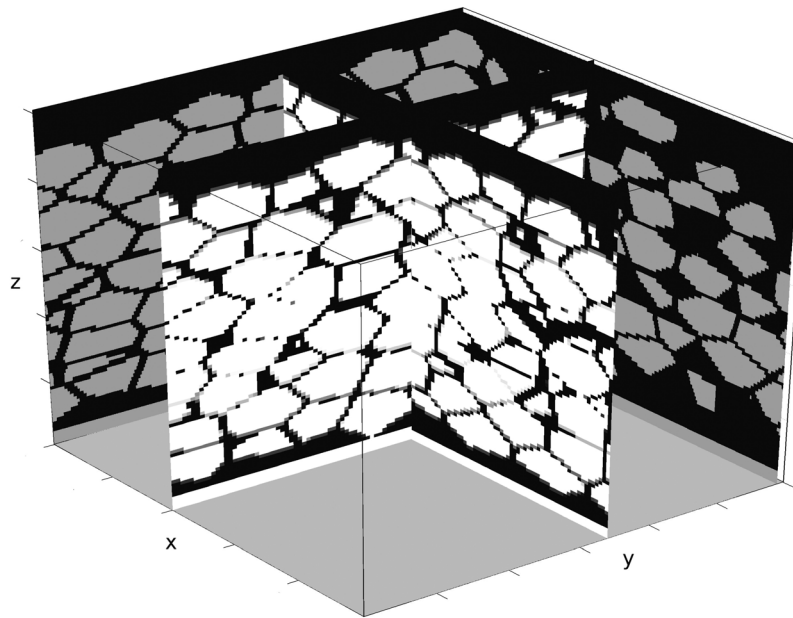


**Figure 2.** Sections through a small volume of simulated granular material (made using the CVT-Halton packing model), in order to visualize the network of pore spaces between grains. The volumetric void fraction in this example is 30%.

all vertices of the particles to touch. This basic simulation of granular material means that at any  $\phi > 0$ , no particles touch and void spaces between adjacent particles are uniform in width. The method therefore requires a modification to the manner in which void spaces are distributed in order to make them more similar to naturally occurring granular materials. This change has particular relevance for uses of simulated granular material as a porous medium.

[18] Adopting the terminology of *Koplik et al.* [1984] for idealized porous media, the network voids consist of approximately cylindrical ‘throats’ connecting the junctions between grains called ‘pores’. In the current modeling approach, all simulations are 3D and have an inherent porosity. Pores, when viewed in section, possess a wide size and shape distribution, but pore throats have approximately equal diameter and scale with bulk porosity. This is likely at odds with many natural sediments. This does not matter if the purpose of simulating particles is to use them in a dynamical model (e.g., granular flow). Nor does it affect the utility of the modeling approach as a means by which to produce simulated sediment surfaces for the purposes of testing automated measurement methods because the surface, as a 2D projection, has no apparent void space because subsurface grains are visible in the void spaces (see the companion paper, part 2). This is because porosity can be modified easily and independent of particle size and shape. Although the micro-geometry of Voronoi cells in 2D have been used in modeling pore space networks relevant to bulk permeability and conductivity characteristics, essentially because the network of pores and throats is random [e.g., *Vrettos et al.*, 1989; *Nagaya and Ishibashi*, 1998], it might however be a limitation if the simulations were to be used for modeling flows through the material.

[19] In order to counter the approximately constant simulated pore throats, one could partially erode a percentage of

grains chosen at random. However, that would increase the bulk porosity of the material and alter the shape distribution in an unknown and uncontrolled manner. A preferable method would therefore be to modify the locations of the particle centers. In its simplest form this could be an addition/subtraction of a random number to 1 or all of the 3 coordinates which define the location of each particle center. This has the effect of moving the grains into or out of previously occupied pore space, thus widening the distribution of pore throat diameters. In practice, this exercise is carried out with a necessary constraint that this does not cause particle overlap. To illustrate the resulting non-uniformity of pore throats, various sections through a simulation with a small number of grains are shown in Figure 2. The percentage of particle locations modified becomes a free parameter. In an application more advanced than carried out here, the spatial uniformity of pores could also be a free parameter (i.e., pore throats are altered according to some spatial density function). This method preserves the shape distribution, and is also carried out in such a way as to preserve the bulk porosity of the material (some pore spaces get larger, others smaller, but the average space remains the same).

[20] The convex hull of points within each Voronoi cell create non-overlapping convex polyhedra with quasi-crystalline faces, and without holes (for a mathematical review of random tessellations see *Møller* [1989]). The Voronoi tessellation is therefore an appropriate model of granular material composed of close packings of individual (discrete) particles, as well as mathematically and computationally simple. *Barndorff-Nielsen* [1989] observed that Voronoi cells would be a suitable model for granular material, and that the range of shapes created are reminiscent of quartz sand particles. Figure 3 shows an example image of quartz sand particles taken with a macro lens. The particle centers have been (somewhat

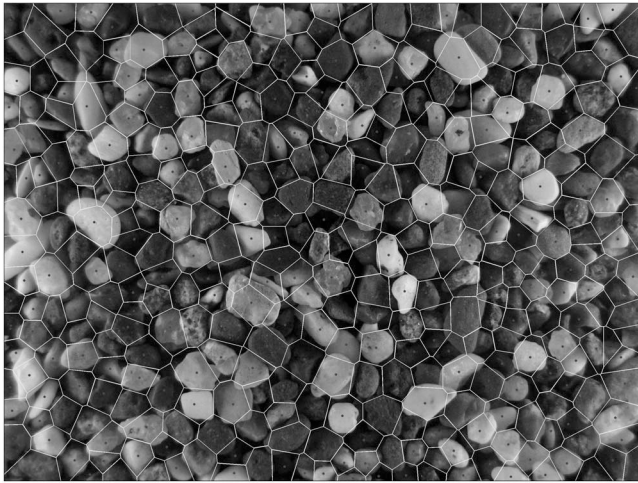


**Figure 3.** Voronoi tessellations as a model for natural granular beds. Particle centers in this photograph of a surface of well-sorted sand have been identified by eye in the image, and the Voronoi tessellation overlain. The tessellation is not a perfect model for the grain outlines, however the statistics of cell area are almost identical to those of apparent particle area. In addition, the shapes of particles are qualitatively similar.

crudely) identified by eye. The Voronoi tessellation for this set of points  $\nu$  is overlain. It is not intended to exactly mimic the structure of grains within the photograph, rather to show the close resemblance in particle size and shape distribution compared with the particles within the image. Instances of over-estimation of particle area are approximately the same in number as instances of under-estimation, so the first-order statistics of area are almost identical.

[21] In this study two types of Voronoi tessellations have been employed, in order to create a greater variety of simulations with respect to granular structure. Other types of Voronoi tessellation [e.g., *Ferenc and Neda, 2007*] could equally be used for further variety. The first we term the Normal Voronoi Tessellation (hereafter NVT), so-called because the generating points do not in general coincide with the particle's center of mass, i.e.,  $z_m \neq z_m^*$  (see review by *Ferenc and Neda [2007]*). The second is the Centroidal Voronoi tessellation (CVT) (see review by *Du et al. [1999]*), where  $z_m = z_m^*$ . Such centroids are computed using the algorithm detailed by *Du et al. [1999]*, which minimizes the integral of the square of the distance between each point in the region ( $x$ ) and its nearest generator ( $z_m$ ).

## 2.2. Geometric Framework: Generating Particle Locations

[22] The modeling framework has been defined in terms of particle and pore generation, but not particle location, which is the subject of this section. By using a Voronoi tessellation approach, particles and the geometric basis for packing are defined entirely by the location of particle centers. The particle centers may be simulated using simple point-generating models called 'processes' which may be statistically homogeneous or inhomogeneous in space, and random or with some degree of determinism in the spatial distribution. All such types are considered here.

[23] Numerous point processes can be used to simulate granular material. As will be shown, different spatial distributions of particle centers create granular simulations with different ensemble properties. An understanding of these properties opens up the opportunity for creating simulations of a specific granular material or tailored to a specific use. Choosing the appropriate point process to create a spatial distribution of particle centers is the simplest and most flexible way to tailor the properties of the simulated granular material to the needs of the user. It is therefore useful to outline and explore the properties of a variety of spatial point processes.

[24] In all cases, increasing numbers of  $\{z_m\}$  are generated in a constant volume in order to simulate granular material composed of finer and finer particles. Hundreds of realizations, a combination of the methods summarized in Figure 4 and containing up to 128,000 discrete particles, have been generated, for each combination of methods, with modest computing power. An example of a simulated granular material with 32,000 particles is shown in Figure 5. The coordinates of each particle center, center of mass, and vertices are known precisely, therefore calculations of volume, surface area, particle contacts (coordination number), and distance to neighboring particles can be made for each particle.

[25] The remainder of this section will be organized with reference to Figure 4 which is a flow diagram of the main options and processes used in this study in order to generate a variety of spatial point distributions. This is, of course, necessarily just a limited subset of algorithms which could be employed in order for the purposes of simulating granular material using a Voronoi tessellation approach. The concepts of NVT and CVT have been introduced in section 2.1. As competing methods through which the particles are created, they can be used in conjunction with spatial distributions generated by any of the methods below. Having decided whether the granular material will be NVT or CVT-based, a decision is made if the point-distribution conforms to an assumed or statistically generated spatial density function (Figure 4). Note that in order to illustrate (in print) the differences in packing structures of the simulated granular material, it is necessary to display 2D sections (Figure 6), but all simulations are 3D unless otherwise stated.

### 2.2.1. Spatial Density Function Generated by Statistical "Rules"

[26] A model for granular material based on a Voronoi tessellation requires a way of generating the set of particle locations, which we term a point process. These point processes are basically statistical rules governing the relative location of collections of points in 3 dimensional space, the Voronoi tessellation of which creates assemblages of cells (particles) with different emergent properties such as particle packing and size distribution. We classify point processes which conform to rules as either 1) spatially homogeneous which, as the name suggests, do not exhibit spatial clustering, or 2) spatially inhomogeneous processes which do cluster.

[27] To illustrate these principles we have limited this study to just three simple homogeneous processes whose quantitative properties are well known, but many more could be considered which would create statistically different assemblages of particles with other packings. The first of the point processes used here is termed a Poisson distribution which uses a random number generator to create coordinates which make up the point distribution (Figure 6a). This,

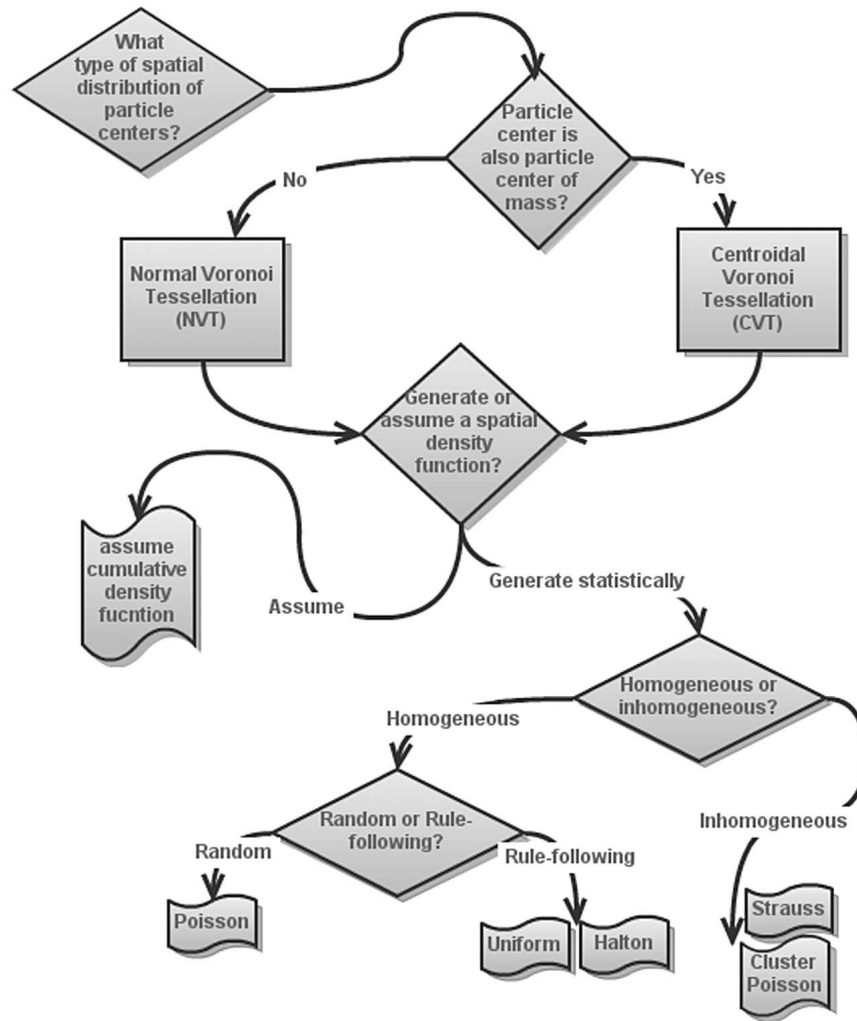


**Figure 4.** Flow diagram summarizing the methods used in this paper for simulating a spatial point distribution with desired characteristics, as detailed in section 2.2.1.

in conjunction with the NVT framework, produces packings which are as non-deterministic as a homogeneous point-generating process will allow (although beds can be less deterministic if the CVT framework or inhomogeneous point-generating processes are used; see below).

[28] In order to simulate significantly differing degrees of order in the packing arrangement of particles, two point-generating processes have been used within the CVT framework. The first, termed CVT-Uniform, begins with a random (Poisson) point distribution and iterates slowly toward a Uniform spatial distribution (i.e., a regular grid). However, it is curtailed after just a few iterations so the resulting beds have a quasi-random structure (Figure 6b). The second point-generating function within a CVT framework (third and last of the homogeneous processes considered here) is the Halton distribution [Halton, 1960], which uses pairs of prime numbers for a base. For example, for the primes 5 and 7 the  $x$  coordinates are created by first dividing the  $\Omega$  by  $5^1, 5^2, \dots, 5^M$ . The CVT-Halton point structure is essentially deterministic and therefore creates synthetic beds containing particles with the most ordered packing arrangements (close to hexagonal; Figure 6c).

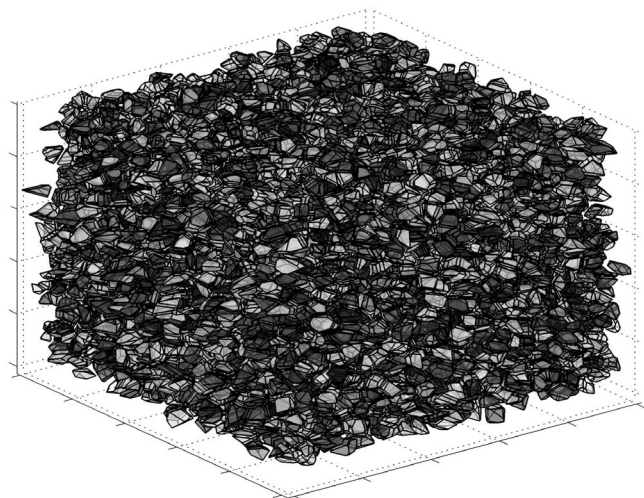


**Figure 5.** Example of a simulated granular material with 32,000 particles in the unit cube. This was generated using a NVT-Poisson approach. Sections through such material are required in order to visualize pore space, e.g., Figure 2.

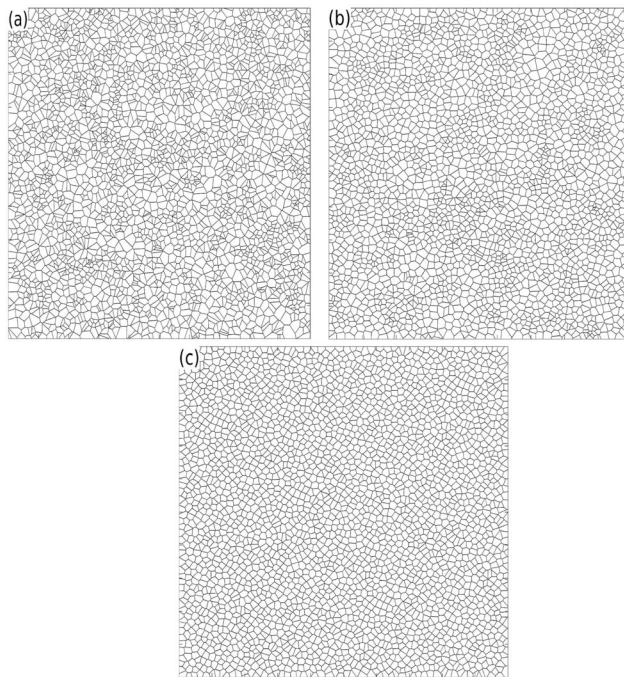


**Figure 6.** Sections through volumes of simulated granular material similar to Figure 5 using the (a) NVT-Poisson; (b) CVT-Uniform; and (c) CVT-Halton underlying spatial point processes. Note that particle packing becomes increasingly more regular (deterministic) (Figures 6a–6c).

[29] The first inhomogeneous process, which we term the Cluster Poisson (CP) model, uses an underlying homogeneous Poisson spatial distribution and adds a clustering mechanism [Martínez and Martínez, 2002]. Adopting the terminology of Bordenave and Torrisi [2007], first a defined number,  $M$ , of ‘parent’ points are generated to form a homogeneous spatial distribution. Then a number of ‘children’ for each parent are generated according to a probability distribution. In this study a Poisson distribution is used with intensity  $\lambda$ , which defines the mean number of children per parent. The relative positions of the children to their parents are independently distributed according to a bivariate distribution. Here we use a bivariate normal distribution that is centered at each parent, but other distribution shapes could be used [e.g., Martínez and Martínez, 2002]. The covariance of the distribution is given by  $\sigma^2 I$ , where  $I$  is an identity matrix and variance  $\sigma^2$  dictates the spread of each cluster around each parent. The points retained in the final spatial pattern are the children only.

[30] Figure 7 shows the number of particles generated by covariation in two free parameters of the CP model, intensity of clustering  $\lambda$  and number of parents,  $M$ . Here, the spread parameter  $\sigma^2$  is fixed. This was constructed empirically by generating sets of point distributions covering this entire parameter space. The effect of increasing  $\sigma^2$  for a given  $M$  and  $\lambda$  is a linear increase in mean particle diameter (Figure 8a), associated with a change in size-distribution shape (Figure 8b). Controlling the shape of the particle size

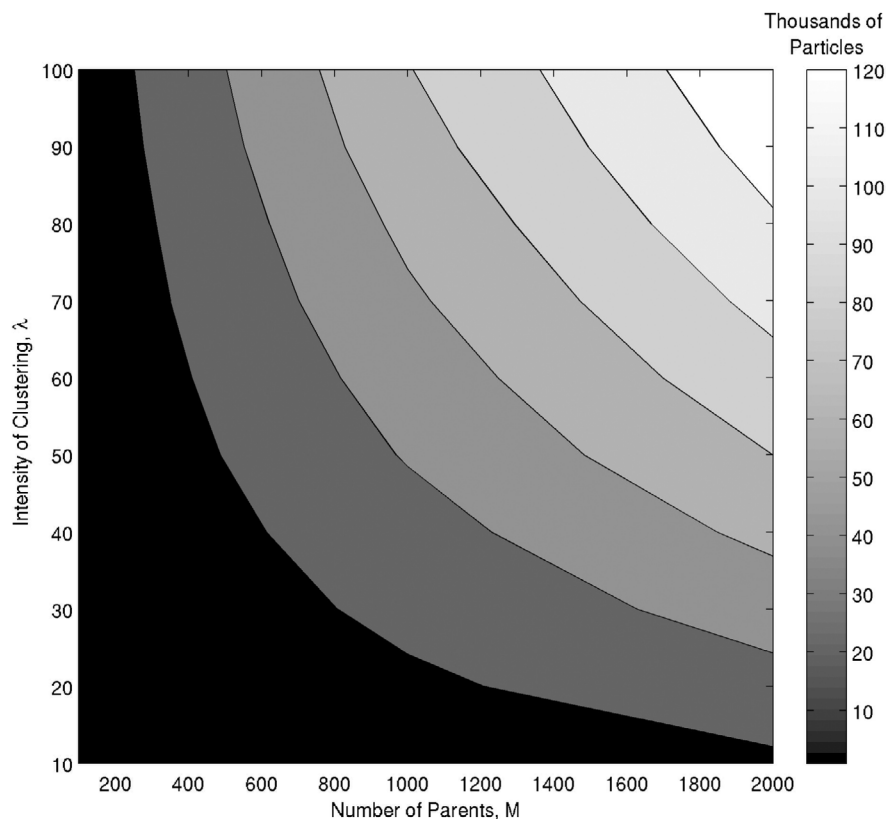


**Figure 7.** Number of particles (shade corresponding to color bar) generated as a function of two free parameters of the CP-model for simulated granular material.  $M$  is the number of ‘parent’ particles and  $\lambda$  is a measure of the clustering around those parent locations. For all cases, a fixed  $\sigma^2 = 0.2$  has been used.

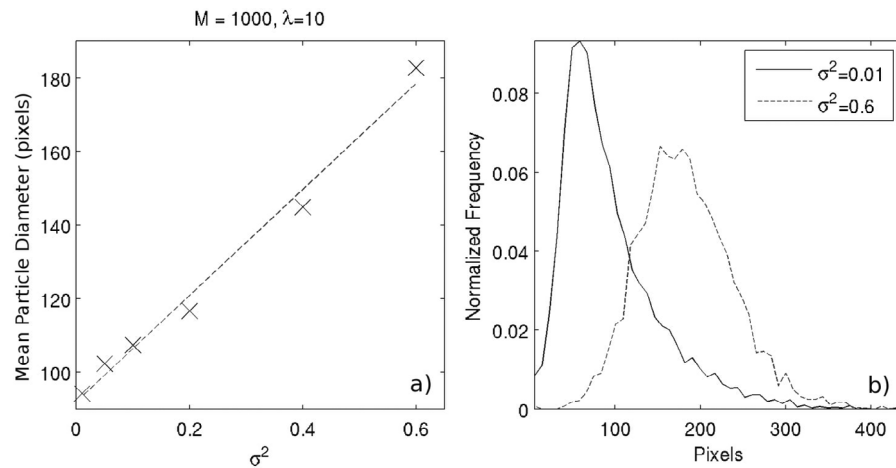


**Figure 8.** Effect of varying  $\sigma$  on (a) particle diameter statistics and (b)  $\mu$  frequency distributions in CP-model generated granular material with fixed  $M = 1000$  and  $\lambda = 10$ .

distribution can be carried out in a consistent manner using the  $\sigma^2$  parameter (Figure 8b). Packing and the statistics of particle size are sensitive to small changes in these parameters, illustrated by Figure 9 which depicts the effects of increasing  $\lambda$  for a given  $\sigma^2$  and  $M$ . For clarity, these are 2D sections through the generated volumes. Size-distributions (and the total number of particles,  $M$ ) are shown for selected sections. While the clustering is quite pronounced, truly bimodal size-distributions are very difficult to achieve using this approach.

[31] The second inhomogeneous spatial point process is the Strauss [Ripley, 1981], the last rule-following inhomogeneous process considered in this contribution. The Strauss model is one where a specified fraction of particle centers is allowed within a distance of any given particle center. Each point is generated in turn using a random number generator, but if there are existing points within radius  $\delta$ , then it is accepted with probability  $c^b$ , where  $c$  is an ‘inhibition’ parameter which specifies the fraction of particle centers allowed within  $\delta$ , and  $b$  represents the number of events already closer than  $\delta$  [Martínez and Martínez, 2002]. A point is therefore accepted if either of the following conditions are satisfied: 1)  $b = 0$ ; or 2) a number randomly generated from a normal distribution  $\leq c^b$ . The process repeats until there are  $M$  particle centers.

### 2.2.2. Spatial Density Function Generated Using an Assumed Random Field

[32] A second means by which particle centers are generated is by creating a random field and utilizing some aspect of that field which varies in space to define a set of points which become the particle centers. This general approach serves as a means to generate a wider range of particle assemblages, beyond those created using some statistical point-generating algorithm as detailed above, with alternate statistics of packing. However, the quantitative properties of generated points may not be well known or mathematically constrained.

[33] One illustration of this approach is to define particle locations using a spatial function over a 3-dimensional region. The magnitude of the values of this function are

unimportant. What is important is the relative spatial locations of peaks and troughs in these values, as defined by some threshold which could, for the present purposes, be either arbitrary or deterministic. Normalizing by the sum of all values, one obtains a discrete probability density function (PDF) associated with each subregion. By assigning an arbitrary order to these subregions, the sum of the PDF subregion is the CDF (cumulative density function) for that subregion. Now given an arbitrary random value  $a$ , the subregion whose CDF value just exceeds  $a$  is located. Sample points are obtained by successively and arbitrarily choosing from within this subregion. Given enough sample points, the statistics for this sample will tend to the input PDF.

[34] To illustrate this process, images having  $1/f$  ( $f =$  frequency) amplitude spectrum properties (known as ‘pink noise’) were generated. Increasing powers of  $f$  create three-dimensional images with greater autocorrelation (larger ‘blobs’). These images were normalized to create a PDF and a point pattern generated consisting of 1000 points distributed according to that PDF. For simplicity we illustrate a random section through a volume of granular material resulting from this process. Figure 10 shows the outputs for (top)  $1/f^5$  noise and (bottom)  $1/f^{0.5}$ , (middle) the point pattern, and (right) the associated Voronoi tessellation. Increasing powers of  $f$  tend to create particles with greater spread in their size-distribution. For example, the  $1/f^5$  spectrum shown in Figure 10 produces a size-distribution with percentiles  $d_{10} = 61, d_{50} = 164, d_{90} = 297$ , compared to the  $1/f^{0.5}$  which produces a size-distribution typified by  $d_{10} = 121, d_{50} = 210, d_{90} = 311$  (all units pixels).

[35] Instead of artificially generating a random field, as above, any suitable existing random field may be used. For example, an image of natural sediment with depositional structures, in this instance as a 2D random field, might also serve as an assumed point density function on which to base the sedimentary simulation. In this case, the basis for the generation of the point distribution are the regions of light and dark shading in the sediment (defined relative to some threshold intensity). For example, Figure 11a depicts the image of a horizontal section through Colorado River sand

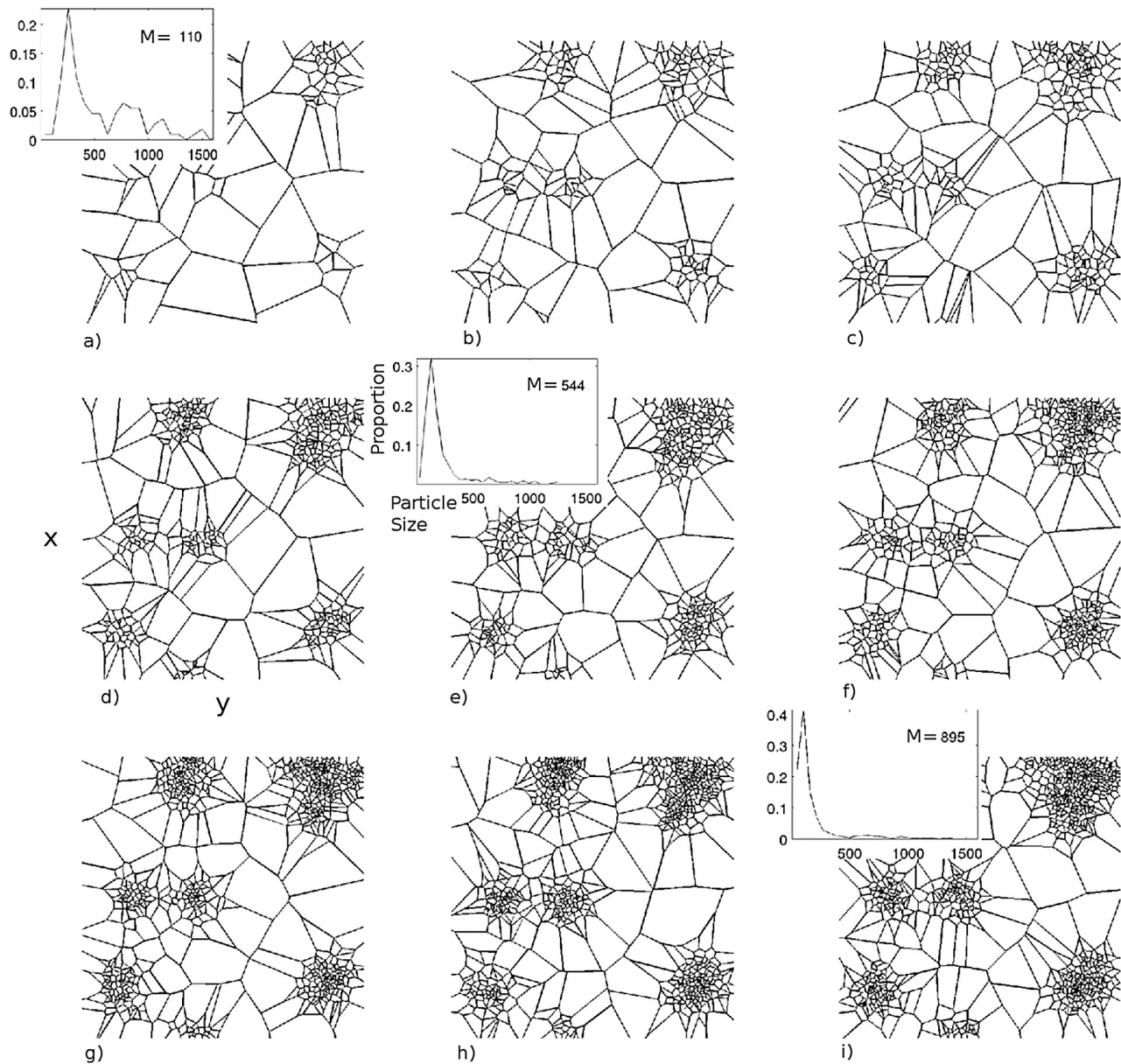


**Figure 9.** Examples of sections through synthetic granular material generated using the CP-model with small numbers of particles (number of particles,  $M < 1000$ ). The intensity of clustering for a given number and location of ‘parents’ (the cluster centers which are identical for all shown simulations) (a–i) increases due to increasing values of the  $\lambda$  parameter (10 to 100), which defines the number of ‘children’ per parent (see text for explanation). The number of parents, about which clustering takes place, is fixed ( $M = 6$ ) as is the spread of the clustering ( $\sigma^2 = 0.2$ ). Example particle size distributions depicted for three example sections (Figure 9a, 9e, and 9i). The smaller the number of particles in a given area, the more tendency to a bimodal distribution, although a truly bimodal distribution is never achieved.

with preserved depositional structures. A region of interest has been selected (Figure 11b) and it has, purely for illustrative purposes, been assumed that the lighter shaded areas contain relatively coarse particles and the darker shaded areas contain fine particles. This image is used to generate a 2D section of sediment by first filtering using a low-pass frequency domain filter on the image to accentuate the contrast in shading, then using this as a spatial PDF in the

same way as the examples above. The point distribution is also generated in the same way using the CDF. The low-pass filtered image is shown in Figure 11c along with the tessellation, in this case representing sectioned particles. Of course, the ‘particles’ in this case are clearly larger than they would be in reality. This was intentionally done, by curtailing the number of generated points to 1000, in order to illustrate the relative size of particles across the image, since

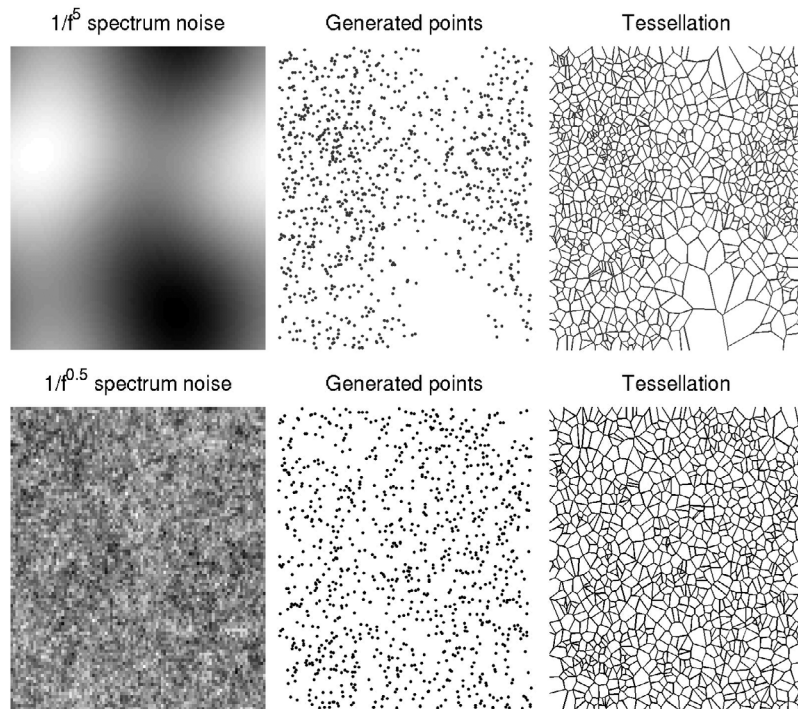


**Figure 10.** Two examples (one per row) of generating a Voronoi tessellation using a random field of  $1/f$  frequency spatial ('pink') noise. Shown in 2D for simplicity but can just as readily be extended to 3D for application in modeling sediment. (top) Larger exponents on  $f$  create autocorrelated 2D surfaces, therefore more inhomogeneous spatial point distributions and their Voronoi tessellations. (bottom) Smaller exponents create more homogeneous spatial distributions and tessellations.

smaller size particles would be difficult to see in print. In reality, however, one would carry on the simulation, perhaps requesting hundreds of thousands of particles.

### 3. Model Performance: Similarities With Natural Granular Material

[36] The modeling approach described here is a general one for creating populations of particles where structural adjustments to packing and fabric have not occurred. In other words, in general the simulated sediments are idealized

and therefore do not contain many of the deterministic structures that might be in real sediment, such as preferred fabric, stratification, imbrication, and porosity that differs with depositional process (for example, greater in grain-flow deposits than wind ripples). In natural sediments packing is the emergent property that results from the forces applied to the particles. The issue of deterministic structures in sediments is often tied up with scope (defined as the ratio of scale to resolution) and population statistics (for example, the ratio of grain size standard deviation to sample volume). The range of particle sizes present in a sample is to some

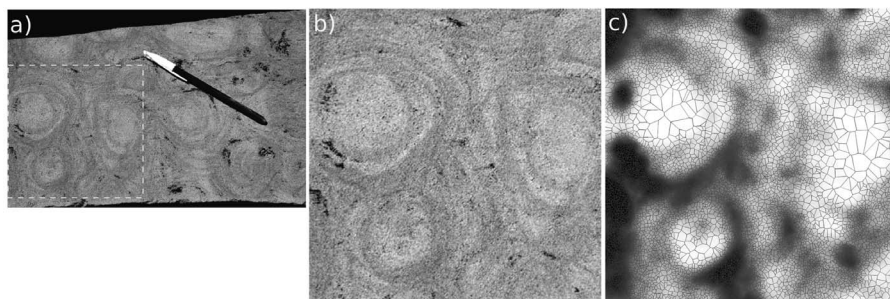


**Figure 11.** (a) Example of a horizontal section through a natural granular material with deterministic depositional structures (in this case formed by stoss-depositional ripples with spurs ([http://walrus.wr.usgs.gov/seds/bedforms/photo\\_pages/pic41.html](http://walrus.wr.usgs.gov/seds/bedforms/photo_pages/pic41.html))); (b) a small section of this image to be used as an assumed random field; (c) a low-pass filtered version of the image overlain by a tessellation based upon a generated a point distribution. Purely for illustrative purposes, in this case it is assumed that the light areas of the original image are relatively coarse particles, and the dark areas are relatively fine particles.

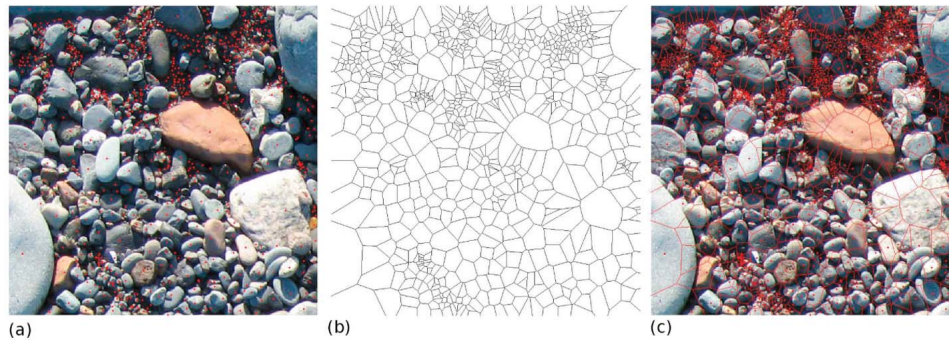


**Figure 12.** (a) Portion of an image of natural granular material exhibiting clustering due, in part, to the presence of many small grains within the interstices of large clasts. A red dot shows approximate particle centers identified by eye; (b) a tessellation based on the spatial point distribution of particle centers shown in a); and (c) the tessellation overlaying the image, showing their agreement. Like in Figure 3, the tessellation is not a perfect model for the grain outlines. In this case the particle size distributions are not as well matched as in Figure 3, underestimating the size of the larger cobbles.

extent a function of that sample volume and also sorting [Church *et al.*, 1987]. For instance, a well-resolved image of fine well-sorted sand may have physical limits of no more than a couple of square centimeters (imposed by the macro-photography) but a sample may adequately capture the variability in the population.

[37] One deterministic structure the model is able to simulate, using an inhomogeneous model for particle centers, is preferential packing of particles in pockets. Graton and Fraser [1935] were among the first to document the process of sand deposition such that the particles (on a microscopic level) are not mutually aligned, which on a macroscopic level produces regions of close packing and adjacent regions of loose packing. Some authors term these proximal regions ‘packing flaws’ [e.g., Prince *et al.*, 1995]. Across a granular surface, the collective effect is a greater ‘clustering’ or apparent spatial segregation of particles based on size/shape. This could be significant if the properties of interest are the distribution of particle contact points, interlocking, seepage/expansion and associated bulk shear resistance properties of the simulated bed. The inhomogeneous processes are therefore more suitable models of granular material with such characteristics (Figure 9). An example physical analog is illustrated by Figure 12 which shows a situation in which clustering of patches of sand due to the placement of gravels and cobbles. The approximate particle centers (identified by dots) have been identified by eye (Figure 12a). The NVT of these points (Figure 12b) produces a cell distribution similar to the outlines of particles, exhibiting the same clustering. A statistically similar result could be achieved using a CP model by seeding it with the locations of  $M$  parents and tuning it with optimal values of  $\lambda$  and  $\sigma^2$  which control the clustering intensity (Figures 7 and 9) and particle size distribution (Figure 8b), respectively. Overlaying the tessellation on the image (Figure 12c) shows that the areal extent of the larger cobbles are systematically under-estimated, providing a clue as to why bi-modality is difficult to achieve (Figure 9): the coarse mode might be consistently under-estimated.

[38] The simulated individual particles are qualitatively (visually) realistic. Much of this is due to the fact that the granular material always has a distribution of sizes and

shapes, and that the particles are convex and contain a number of planar faces (approximately 15 is the average for a 3D particle) separated by straight edges which gives them a quasi-crystalline appearance. The approaches described here are able to create populations of particles with size-distributions which are log-hyperbolic in form (Figure 13) (these were fitted using the maximum-likelihood estimation method detailed by Buscombe *et al.* [2010]). In fact, particle size-distributions are almost perfectly modeled by a log-hyperbolic probability density function when the number of particles measured exceeds 1000, irrespective of particle packing, shape, and degree of homogeneity in the underlying spatial arrangement of particle centers. The log-hyperbolic is a family of heavy-tailed distributions which includes the normal and lognormal as limiting cases, and which has been suggested as the ‘universal form’ of natural size-distributions [Barndorff-Nielsen, 1977; Bagnold and Barndorff-Nielsen, 1980]. See Fieller *et al.* [1992] for a comprehensive review of the statistical form of particle size-distributions.

[39] Due to the irregular tessellation, the particles have convex shapes (i.e., the facets do not inwardly converge) which is also generally true of naturally occurring clastic particles. Particle sphericity is defined, where  $A_p$  is the surface area of the particle, as [Wadell, 1935]:

$$S = \frac{\pi^{1/3} (6V_p)^{2/3}}{A_p}. \quad (4)$$

[40] The distribution of particle sphericities (Figure 14) indicates that the particles have a range of regular and quasi-regular polyhedron shapes such as tetrahedra, octahedra, icosahedra, and dodecahedra, i.e., a quasi-crystalline structure. Natural particles tend to have sphericities in the range 0.7 to 1 [Cho *et al.*, 2006]. In the simulations presented here, mean  $S$  is approximately 0.87 for all NVT- and CVT-based simulations; 0.75–0.78 for Strauss-based simulations; and 0.65–0.8 for various CP-based simulations.

[41] Perhaps the simplest way to control the porosity of the simulated granular material is by shrinking or expanding each vertex of each of the cells by a uniform amount (to a

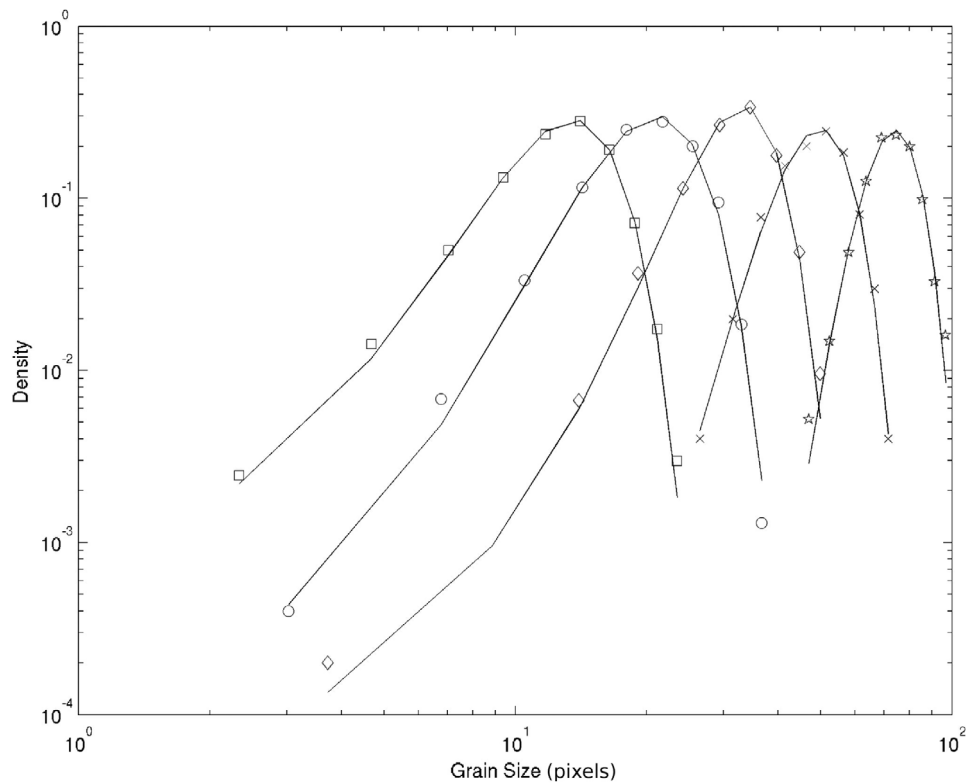


**Figure 13.** The particle size-distributions of granular sections generated using a Halton CVT point density (symbols), for images containing 2500 (stars), 5000 (crosses), 10000 (diamonds), 20000 (circles), and 40000 (squares) particles, and their log-hyperbolic fits (solid lines). The log-hyperbolic model enjoys a similar good fit to data from NVT and CVT-Uniform based synthetic sediment beds.

limit to prevent particle overlap). If  $E$  are the extreme points of the vertices (coordinates relative to the origin) of each particle in each direction,  $F$  is the reduction factor, and the overline represents the mean, each vertex can be reduced using:

$$E_r = FE + (1 - F)\bar{E}. \quad (5)$$

[42] For example, for a 90% reduction in each particle volume,  $F = 0.1$  and for a 20% reduction  $F = 0.8$ . In this way the porosity increases and the particle size decreases, each by the prescribed amount, but particle shape remains the same. This is different from particle (morphological) erosion which would affect particle shape and cause unknown changes to the particle size-distribution.

[43] The effect of a given  $F$  on void ratio ( $e = \nabla_v / \nabla_p$ ) varies with mean particle size. In order to make the simulations as realistic as possible to natural sediments, the porosity of the simulations was controlled, using the  $F$  parameter, in order to fit observed bi-variation of  $e$  and  $S$  in experimental data. The data set chosen was that of *Cho et al.* [2006], which consists of 37 types of granular material, including crushed and natural sands, glass beads and granite powder.

[44] There exists an optimal  $F$  which makes the bi-variation of  $e$  and mean  $S$  (Figure 15) conform to the empirical relationship found by *Cho et al.* [2006] for natural sediments. Particles generated using the NVT-, CVT- and Halton

tessellations have mean sphericities between 0.87–0.9 which, according to *Cho et al.* [2006], means  $e$  is approximately 0.85 ( $\nabla_v = 0.54$ ). Those particles generated using cluster point processes have mean sphericities between 0.65 and 0.8. To put these values in context, the void ratio for uncompacted sediments is about 0.85 for well sorted, 0.67 for moderately sorted, and 0.25 for extremely poorly sorted [*Terzaghi et al.*, 1996]. Optimal  $F$  depends on the model used and the number of particles, increasing as a function of the number of particles for granular material based on inhomogeneous point distributions, and decreasing for homogeneous point distributions (Figure 15, right). The correct relationship between  $e$  and  $S$  (Figure 15, left) is very sensitive to  $F$ , which therefore constitutes a very important part of the model.

[45] The modification of particle concentration in order to preserve the sphericity-void ratio relationship is the last part of the process of simulating granular material used in this study, which has been summarized in schematic form in Figure 16. It describes the work-flow from choosing a model to generate particle centers (section 2.2, encompassing the decisions made regarding their spatial characteristics, as illustrated by Figure 4) to creating the basic cell population using a NVT or CVT Voronoi tessellation (section 2.1). Then the optional modification is made to pore throat geometries, as described in section 2.1. Finally, it describes the application of an optimal  $F$  to preserve observed variation of average particle sphericity and void ratio (Figure 15). Note

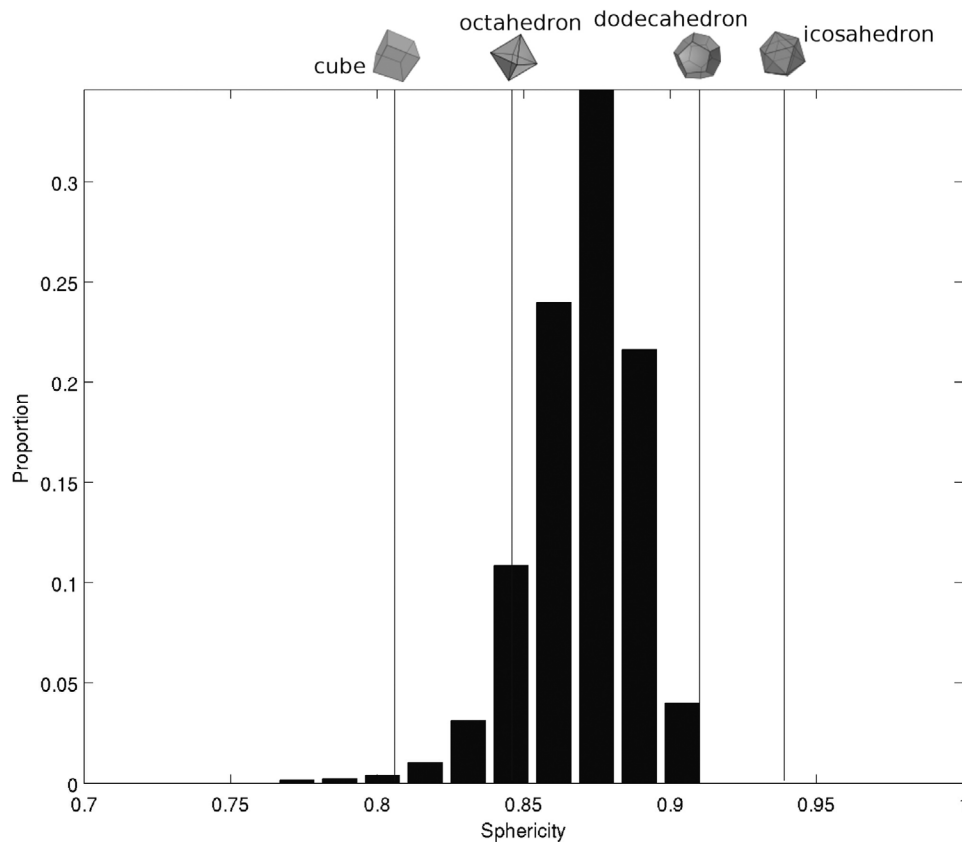


**Figure 14.** Typical shape-distribution of the simulated sediments using an homogeneous packing model. The shape metric is sphericity, calculated using particle volumes and surface areas. Values between 0.7 and 1 are typical of naturally occurring particles [Cho *et al.*, 2006]. The values of this metric for common polyhedra are shown for reference.

this procedure does not affect the pore throat geometries, being a uniform operation on all grain volumes.

#### 4. Discussion

[46] Simple stochastic models have traditionally been used to generate models of granular material. These often use a binary random field approach which treats the granular material as two phases of matter (solid particles and gas- or fluid-filled ‘voids’) by simulating only the solid phase [e.g., Fara and Scheidegger, 1961; Preston and Davis, 1976; Sen, 1984; Koutsourelakis and Deodatis, 2005; Buscombe *et al.*, 2010]. In such an approach, the particle geometries and packing characteristics at the scale approaching the individual grains are unrealistic even if the bulk properties such as porosity are adequately simulated. Geometric methods essentially take the reverse approach by first defining an elementary shape (usually idealized such as a sphere) with or without a distribution of sizes, and arrange them into a bed in such a way which may inadequately replicate the bulk properties such as packing [e.g., Bernal and Mason, 1960; Potapov and Campbell, 1998; Latham and Munjiza, 2004].

[47] The approach taken here is different because it uses a stochastic model to create points (particle centers) about which geometric objects (particles) are created based on the random subdivision of space. The location, size and shape of these particles are defined the instant that subdivision

(tessellation) is made. Thereby the simulated beds have a structure which is related to the spatial distribution of the particle centers.

[48] The model has particle size and shape emerge from initial placement of particle centers, which is at odds with natural sediment beds, in which the sediment size and shape are pre-determined. However, the size-, shape- and pore-space distributions of resulting simulated granular materials are similar to those of natural well-sorted sediments. The inherent three-dimensionality of the resulting discrete particle model eliminates the requirement for a (somewhat complicated) stereology. In addition, the pre-determination of a random distribution of particle centers as a stochastic process with a clearly defined mathematical description, a lack of which has hampered theoretical studies of densely packed granular material to date given that the particles cannot overlap [Moran, 1966; Kellerhals *et al.*, 1975], allows the model to potentially provide a mathematical basis to variations in sediment packing and structure.

[49] We have used two types of Voronoi tessellation, namely the classic or NVT (equation (2)) and the centroidal or CVT (equation (3)). In addition, a radical (or Laguerre) Voronoi tessellation could be used, which weights the cell boundaries according to the relative diameter of the particles. Such an approach might be useful for simulating particles with a greater standard deviation in particle size [Gervois *et al.*, 2002]. All model realizations presented here

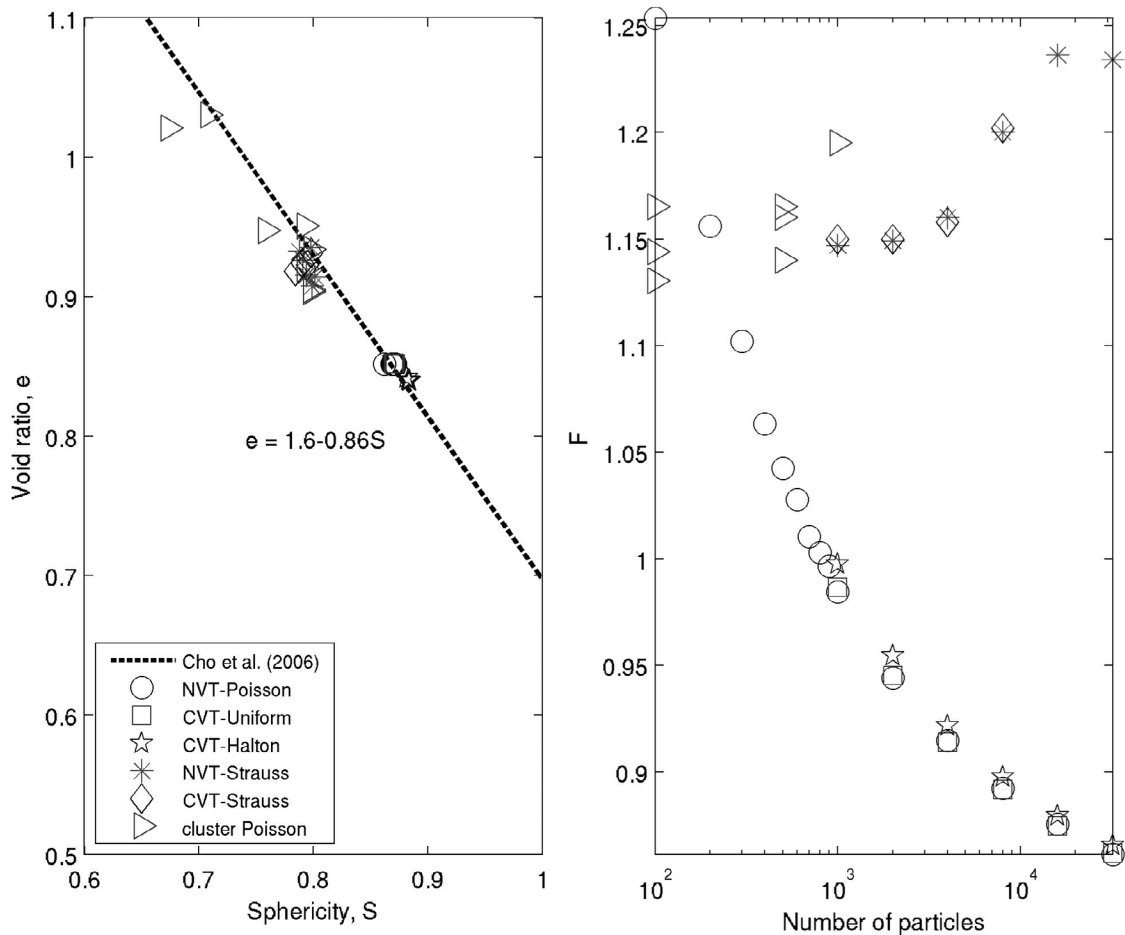


**Figure 15.** Left: comparison of particle characteristics compared to natural particles. The dashed line is the sphericity versus void ratio empirical relationship of *Cho et al.* [2006] (equation). The symbols represent the corresponding points for various packing models employed in this study, indicating a range in this parameter space. Right: the particle concentration factor,  $F$ , required to achieve the close approximations seen in the sphericity versus void ratio relationship in the left panel.  $F$  is an increasing function of the number of particles for inhomogeneous packing structures (asterisks, diamonds, triangles), and a decreasing function of the number of particles for homogeneous packing structures (circles, squares, stars).

are based on the point distributions whose distributions are completely determined by their mean and covariance [Ripley, 1981]. It appears that competing spatial point processes such as a Gibbs point distribution [Mase, 1986] do not produce tessellations whose cells have such heavy distribution tails [Barndorff-Nielsen, 1989] so these processes were not considered further in this study. The observation that the log-hyperbolic density is universally applicable to size-distributions of the granular materials simulated here supports a long-held belief [Barndorff-Nielsen, 1977; Bagnold and Barndorff-Nielsen, 1980]. However, it might also suggest that the log-hyperbolic form of particle size-distributions has a geometric basis rather than a dynamic explanation, as proposed by Bagnold and Barndorff-Nielsen [1980] and Barndorff-Nielsen and Christiansen [1988], but which has not been universally accepted by sedimentologists. Models which generate tessellations with specified size-distributions invoke more complicated spatial point process with more rules and attractive forces [Mürmann, 1978] or use genetic algorithms [Suzudo and Kaburaki, 2009].

However, it would be even more difficult to generate realistic packings of particles with both pre-defined size-distributions and pre-defined shape-distributions. In addition, these methods are very computationally intensive.

[50] It is beyond the scope of this paper to examine in great detail all possible permutations of sedimentary variety allowed by this modeling approach. However, a number of different approaches have been detailed (Figure 4) which result in geometries/packings which are sufficiently different as to affect, for a given number of requested particles, bulk statistics such as mean particle size, shape, etc. This is remarkable given the large numbers of particles involved, plus the fact that the only control on the structure of the bed is the placement of particle centers. Point-generating stochastic models such as the CP and Strauss models described in section 2.2.1 have a number of free parameters which combine to define the degree of point clustering and other aspects of granular structure. The more free parameters in such a rule-following approach, perhaps the greater likelihood of generating a wider spectrum of packing arrangements.

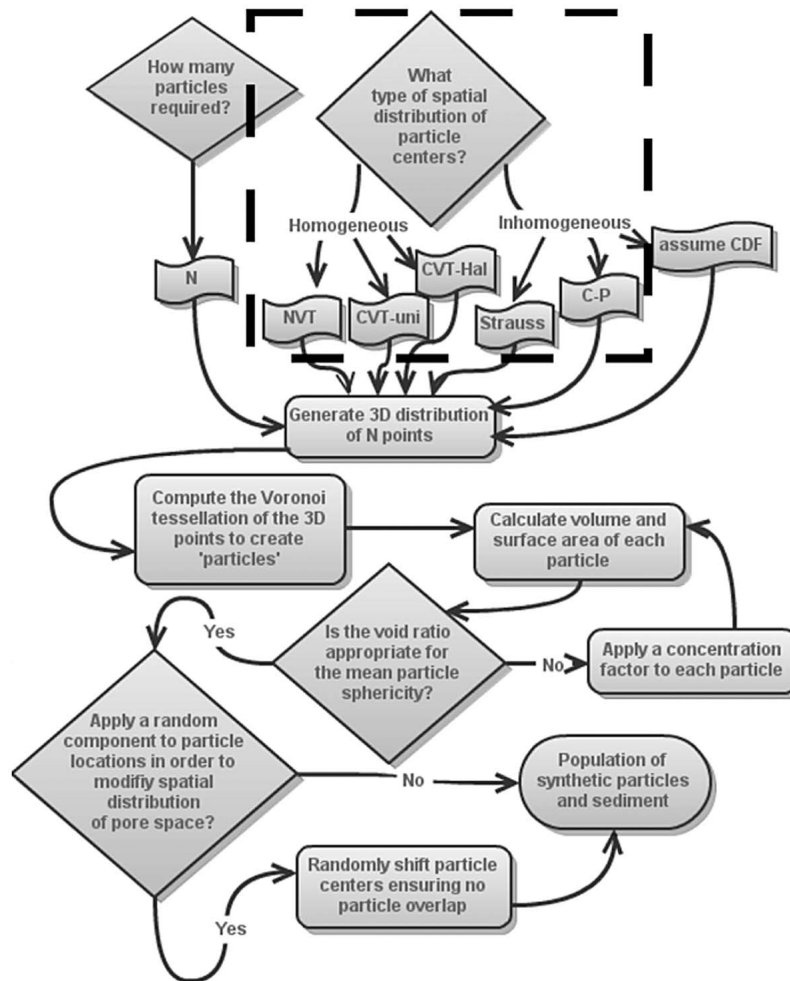


**Figure 16.** Flow diagram summarizing the methods used in this paper for simulating granular matter. The dashed box represents the part of the algorithm illustrated in more detail in Figure 4.

However, more parameters might also make the mathematical description of such point distributions (and indeed tessellations based upon them) more complex.

[51] The simulated sedimentary structures range from purely stochastic to weakly deterministic (clustering of packed particles), thus the modeling approach detailed here is not able to simulate all types of natural sediment, especially those with any deterministic structures which are the result of physical sedimentation processes. Rather, it has been designed to simulate populations of relatively well-sorted granular material. The model is only able to simulate a subset of sediment structures. Indeed, deterministic structures in the simulated sediments are not possible in this modeling framework. In order to simulate a particular deterministic structure in sediment one would need two models: 1) a model to generate a population of 3D particles with realistic and known size-distribution and a range of realistic shapes (a ‘static’ model such as detailed here); and 2) a deterministic physics-based model which uses the discrete 3D particles to simulate depositional processes creating the deterministic structures of interest (a ‘dynamic’ model). Such so-called Discrete Particle Models, which resolve the contact forces between individual grains as well as momentum exchanges between individual particles and

the transporting fluid in a Lagrangian framework, are becoming increasingly popular methods by which the dynamics of granular [e.g., *Latham and Munjiza, 2004*] and fluid-granular flows [e.g., *Schmeeckle and Nelson, 2003*] are understood.

[52] The ability of the model to simulate a specific naturally occurring sediment would be influenced by errors in both the realism of the population of particles generated by the ‘static’ model, and the adequacy of the physics encapsulated in the ‘dynamic’ model. Therefore, a reasonable evaluation of the performance of the proposed modeling approach must be limited to the former, i.e., comparing statistical measures of simulated and natural populations of particles. We will therefore limit our contribution to simulation of a given sediment through the description of generating simulated particles with a packing defined according to some assumed random field given in section 2.2.2 (Figure 11). In the present section the general form of simulated particle size and shape distributions are compared to those found in nature. A further step in the simulation process is described whereby the bi-variation of particle shape (sphericity) and porosity found in natural unconsolidated clastic particles is preserved.

[53] In this modeling approach we see no theoretical constraints with increased particle size variability with scale,

thereby simulating a square-meter image of gravels and sands equally well as a square-kilometer image of boulders, gravels and sands, and so on. At large scales, computational issues would arise with simulating very large volumes. This, and the issues of deterministic structures, have dictated that the model has been designed to simulate relatively small (up to millions of particles) volumes of relatively well-sorted granular material.

[54] In the second of this pair of papers (part 2) this modeling approach is used to generate many realizations of granular materials to develop and test automated methods for quantifying particle-size statistics from images of surfaces of natural sediment. The model is used to test methods designed to estimate the apparent grain sizes of the surface (granulometry), and also to infer vertical distribution of grain sizes within planar samples through the surface layers of the sediment (coined *unfolding* by Ripley [1981]) in order to quantify the likely mismatch between the apparent and actual particle size of the surface population of particles.

[55] While our primary aim is to simulate collections of mineralogical particles (sedimentary clasts), the modeling approach described here may provide an alternative model for non-mineralogical granular material such as foam, aggregations of biological cells and seeds, chemical crystals, as well as non-natural granular material such as manufactured products (e.g., bearings, pharmaceuticals, etc). Such materials will have very different deterministic structures.

[56] In sedimentology, the modeling approach detailed here, in the field of computed tomography for quantitative characterization of natural sediments [e.g., Holler and Kogler, 1990] might aid the interpretation and representation in idealized forms of well-sorted sediments for further use in theoretical and simulation-based studies. In addition, granular simulations such as these may complement recent advances made in the direct measurement of the packing properties of sand [e.g., Louge et al., 2010].

## 5. Conclusion

[57] Models of granular material which do not use regular geometrical shapes (such as spheres) for the elementary particle are more realistic representations of a variety of naturally occurring granular material. However, traditionally such material has been difficult to simulate through computationally simple means, as well as difficult to ascribe a mathematical basis to variations in sediment packing and structure. Here, a new framework for the simulation of natural granular material has been explored based on the principle of Voronoi tessellation. Variations in particle size and packing can be achieved simply by varying the spatial point distribution about which the Voronoi cells (particles) are constructed. Such point distributions, and therefore the simulated sediment, have a well known mathematical basis if generated using a spatial point-generating stochastic model.

[58] This approach is both theoretically and practically simple, and creates populations of qualitatively realistic particles with size and shape distributions (specifically, lognormal and log-hyperbolic) conforming quantitatively to those found in a great variety of natural sediments. In addition, the simulated materials mimic particle sphericities and porosities within known values. However, the three-dimensional

packings of these particles simulate rather idealized sediments which lack the deterministic structures common in natural sediments. One would therefore require a dynamic physics-based discrete particle model to replicate the more deterministic sedimentary structures found in nature. The primary advantages of using the methods detailed here for generating the population of particles, compared to traditional approaches, would be the realism of the particles and the computational simplicity. As such, the modeling approach detailed here might readily replace spheres and other regular shapes, with limited or no distribution of particle size, in forming the basis of direct numerical simulations of fluid-granular flows or indeed pore water flows through the material. The structure and images of the surface layers of simulated granular materials have been used to evaluate new automated methods for measurement of particle size and structure, which is the subject of the companion paper.

[59] **Acknowledgments.** This work was started while the first author was a postdoctoral research fellow at the United States Geological Survey (Western Coastal and Marine Geology) and the Institute of Marine Studies, University of California, Santa Cruz. Thanks to Jon Warrick for the image used in Figure 12. Thanks to Alex Nimmo-Smith, Chris Sherwood, Jingping Xu, Patrice Carbonneau, and two anonymous reviewers for their constructive comments. Sediment simulation code is available from the first author. The computational geometry algorithms of M. Kvasnica et al. (unpublished data, Multi-parametric toolbox, <http://control.ee.ethz.ch/~mpt/>, 2004) were used for the display, sectioning and volumetric calculations.

## References

- Bagnold, R., and O. Barndorff-Nielsen (1980), The pattern of natural size distributions, *Sedimentology*, 27, 199–207.
- Barnard, P., D. Rubin, J. Harney, and N. Mustain (2007), Field test comparison of an autocorrelation technique for determining grain size using a digital ‘beachball’ camera versus traditional methods, *Sediment. Geol.*, 201, 180–195.
- Barndorff-Nielsen, O. (1977), Exponentially decreasing distributions for the logarithm of particle size, *Proc. R. Soc. London, Ser. A*, 353, 401–419.
- Barndorff-Nielsen, O. (1989), Sorting, texture, and structure, *Proc. R. Soc. Edinburgh*, 96, 167–179.
- Barndorff-Nielsen, O., and C. Christiansen (1988), Erosion, deposition, and size distributions of sand, *Proc. R. Soc. London, Ser. A*, 417, 335–352.
- Bear, J. (1972), *Dynamics of Fluid in Porous Media*, Dover, New York.
- Bernal, D., and J. Mason (1960), Coordination of randomly packed spheres, *Nature*, 188, 910–911.
- Bordenave, C., and G. Torrisi (2007), Large deviations of Poisson cluster processes, *Stochastic Models*, 23, 593–625.
- Buscombe, D. (2008), Estimation of grain-size distributions and associated parameters from digital images of sediment, *Sediment. Geol.*, 210, 1–10.
- Buscombe, D., and G. Masselink (2009), Grain size information from the statistical properties of digital images of sediment, *Sedimentology*, 56, 421–438.
- Buscombe, D., and D. M. Rubin (2012), Advances in the simulation and automated measurement of well-sorted granular material: 2. Direct measures of particle properties, *J. Geophys. Res.*, 117, F02001, doi:10.1029/2011JF001975.
- Buscombe, D., D. M. Rubin, and J. A. Warrick (2010), A universal approximation to grain size from images of non-cohesive sediment, *J. Geophys. Res.*, 115, F02015, doi:10.1029/2009JF001477.
- Carbonneau, P., S. Lane, and N. Bergeron (2004), Catchment-scale mapping of surface grain size in gravel bed rivers using airborne digital imagery, *Water Resour. Res.*, 40, W07202, doi:10.1029/2003WR002759.
- Carbonneau, P., N. Bergeron, and S. Lane (2005), Automated grain size measurements from airborne remote sensing for long profile measurement of fluvial grain sizes, *Water Resour. Res.*, 41, W11426, doi:10.1029/2005WR003994.
- Cho, G.-C., J. Dodds, and J. Santamarina (2006), Particle shape effects on packing density, stiffness, and strength: Natural and crushed sands, *J. Geotech. Geoenviron. Eng.*, 132, 591–602.
- Church, M. A., D. G. McLean, and J. F. Wolcott (1987), *River bed gravels: Sampling and analysis*, in *Sediment Transport in Gravel-Bed Rivers*, edited by C. R. Thorne, J. C. Bathurst, and R. D. Hey, John Wiley, New York.

- Drake, T., and J. Calantoni (2001), Discrete-particle model for sheet flow sediment transport in the nearshore, *J. Geophys. Res.*, *106*, 19,859–19,868, doi:10.1029/2000JC000611.
- Du, Q., V. Faber, and M. Gunzburger (1999), Centroidal Voronoi Tessellations: Applications and algorithms, *SIAM Rev.*, *41*, 637–676.
- Fara, H. D., and A. E. Scheidegger (1961), Statistical geometry of porous media, *J. Geophys. Res.*, *66*, 3279–3284, doi:10.1029/JZ066i010p03279.
- Favier, J., M. Abbaspour-Fard, M. Kremmer, and A. Raji (1999), Shape representation of axi-symmetrical, non-spherical particles in discrete element simulation using multi-element model particles, *Eng. Comput.*, *16*, 467–480.
- Ferenc, J.-S., and Z. Neda (2007), On the size distribution of Poisson Voronoi cells, *Physica A*, *385*, 518–526.
- Fieller, N., E. Flenley, and W. Olbricht (1992), Statistics of particle size data, *Appl. Stat.*, *41*, 127–146.
- Gervois, A., L. Oger, P. Richard, and J. P. Troadec (2002), Voronoi and radical tessellations of packings of spheres, *Computat. Sci.*, *2331*, 95–104.
- Ghaboussi, J., and R. Barbosa (1990), Three-dimensional discrete element method for granular materials, *Int. J. Numer. Anal. Methods Geomech.*, *14*, 451–472.
- Graham, D., I. Reid, and S. Rice (2005), Automated sizing of coarse-grained sediments: Image processing procedures, *Math. Geol.*, *37*, 1–28.
- Graton, L., and H. Fraser (1935), Systematic packing of spheres with particular relation to porosity and permeability, *J. Geol.*, *43*, 885–909.
- Gretzen, R., and R. Levey (1982), Rigid-peel technique for preserving structures in coarse-grained sediments, *J. Sediment. Petrol.*, *52*, 652–654.
- Halton, J. (1960), On the efficiency of certain quasi-random sequences of points in evaluating multi-dimensional integrals, *Numer. Math.*, *2*, 84–90.
- Holler, P., and F. Kogler (1990), Computer tomography: A nondestructive, high-resolution technique for investigation of sedimentary structures, *Mar. Geol.*, *91*, 263–266.
- Ingle, J. (1966), *The Movement of Beach Sand*, *Dev. in Sedimentol.*, vol. 5, 221 pp., Elsevier, New York.
- Jensen, R., P. Bosscher, M. Plesha, and T. Edil (1999), DEM simulation of granular media-structure interface: Effect of surface roughness and particle shape, *Int. J. Numer. Anal. Methods Geomech.*, *23*, 531–547.
- Jodrey, W., and E. Tory (1979), Simulation of random packing of spheres, *J. Simul.*, *21*, 1–12.
- Kellerhals, R., J. Shaw, and V. Arora (1975), On grain size from thin sections, *J. Geol.*, *83*, 79–96.
- Koplik, J., C. Lin, and M. Vermette (1984), Conductivity and permeability from microgeometry, *J. Appl. Phys.*, *56*, 3127–3131.
- Koutsourelakis, P.-S., and G. Deodatis (2005), Simulation of binary random fields with applications to two-phase random media, *J. Eng. Mech.*, *131*, 397–412.
- Latham, J., and A. Munjiza (2004), The modelling of particle systems with real shapes, *Philos. Trans. R Soc.*, *362*, 1953–1973.
- Lin, C. (1982), Microgeometry I: Autocorrelation and rock microstructure, *Math. Geol.*, *14*, 343–360.
- Louge, M., A. Valance, A. Ould el-Moctar, and P. Dupont (2010), Packing variations on a ripple of nearly monodisperse dry sand, *J. Geophys. Res.*, *115*, F02001, doi:10.1029/2009JF001384.
- Martínez, W. L., and A. R. Martínez (2002), *Computational Statistics Handbook With MATLAB*, Chapman and Hall, Boca Raton, Fla.
- Mase, S. (1986), On the possible form of size distributions for Gibbsian processes of mutually non-intersecting balls, *J. Appl. Probab.*, *23*, 646–659.
- Mehta, A. (2007), *Granular Physics*, Cambridge Univ. Press, New York.
- Møller, J. (1989), Random tessellations in  $R^d$ , *Adv. Appl. Probab.*, *21*, 37–73.
- Moran, P. (1966), A note on recent research in geometrical probability, *J. Appl. Probab.*, *3*, 453–463.
- Moscinski, J., and M. Bargiel (1991), C-language program for the irregular close packing of hard spheres, *Comp. Phys. Commun.*, *64*, 183–192.
- Mürmann, M. (1978), Poisson point processes with exclusion, *Z. Wahrsch. verw. Geb.*, *43*, 23–37.
- Nagaya, T., and Y. Ishibashi (1998), Effective medium approximation in Voronoi network systems, *Jpn. J. Appl. Phys.*, *37*, 157–160.
- Neupauer, R., and K. Powell (2005), A fully anisotropic Morlet wavelet to identify dominant orientations in a porous medium, *Comp. Geosci.*, *31*, 465–471.
- Potapov, A., and C. Campbell (1998), A fast model for the simulation of non-round particles, *Granular Matter*, *1*, 9–14.
- Preston, F. W., and J. C. Davis (1976), Sedimentary porous materials as a realization of a stochastic process, in *Random Processes in Geology*, edited by D. F. Merriam, pp. 63–86, Springer, New York.
- Prince, C., R. Ehrlich, and Y. Anguy (1995), Analysis of spatial order in sandstones II: Grain clusters, packing, flaws, and the small-scale structure of sandstones, *J. Sediment. Res.*, *65*, 13–28.
- Ripley, B. (1981), *Spatial Statistics*, Wiley, London.
- Rubin, D. (2004), A simple autocorrelation algorithm for determining grain size from digital images of sediment, *J. Sediment. Res.*, *74*, 160–165.
- Rubin, D. M., D. Topping, H. Chezar, H. Hazel, J. Schmidt, M. Breedlove, T. Melis, and P. Grams (2010), 20,000 grain-size observations from the bed of the Colorado River, and implications for sediment transport through the Grand Canyon, paper presented at 9th Federal Interagency Sediment Conference, Eng. Res. and Dev. Cent., Las Vegas, Nev.
- Schmeeckle, M., and J. Nelson (2003), Direct numerical simulation of bed-load transport using a local, dynamic boundary condition, *Sedimentology*, *50*, 279–301.
- Sen, Z. (1984), Autorun analysis of sedimentary porous materials, *Math. Geol.*, *16*, 449–463.
- Suzudo, T., and H. Kaburaki (2009), An evolutionary approach to the numerical construction of polycrystalline structures using the Voronoi tessellation, *Phys. Lett. A*, *373*, 4484–4488.
- Terzaghi, K., R. Peck, and G. Mesri (1996), *Soil Mechanics in Engineering Practice*, 3rd ed., John Wiley, New York.
- Torabi, A., H. Fossen, and B. Alaei (2008), Application of spatial correlation functions in permeability estimation of deformation bands in porous rocks, *J. Geophys. Res.*, *113*, B08208, doi:10.1029/2007JB005455.
- Tovey, N., and M. W. Hounslow (1995), Quantitative micro-porosity and orientation analysis in soils and sediments, *J. Geol. Soc. London*, *152*, 119–129.
- Van den Berg, E., A. Meesters, J. Kenter, and W. Schlager (2002), Automated separation of touching grains in digital images of thin sections, *Comp. Geosci.*, *28*, 179–190.
- Vrettos, N., H. Imakoma, and M. Okazaki (1989), An effective medium treatment of the transport properties of a Voronoi tessellated network, *J. Appl. Phys.*, *66*, 2873–2878.
- Wadell, H. (1935), Volume, shape, and roundness of quartz particles, *J. Geol.*, *43*, 250–280.
- Warrick, J. A., D. M. Rubin, P. Ruggiero, J. Harney, A. E. Draut, and D. Buscombe (2009), Cobble cam: Grain-size measurements of sand to boulder from digital photographs and autocorrelation analyses, *Earth Surf. Processes Landforms*, *34*, 1811–1821.

D. Buscombe, School of Marine Science and Engineering, University of Plymouth, Plymouth PL4 8AA, UK. (daniel.buscombe@plymouth.ac.uk)

D. M. Rubin, United States Geological Survey, Santa Cruz, CA 95060, USA. (drubin@usgs.gov)